Structural and electrical properties of Sm^{3+} DOPED Co- Zn Ferrite

Kadam G.B., Shelke S.B. and Jadhav K.M.
Department of Physics, Dr. Babasaheb Ambedkar Marathwada University, Aurangabad

Abstract- Polycrystalline ferrite samples having the general formula Co_{1-x} Zn_x $Fe_{2-y}Sm_yO_4$ (where x= 0.0,0.1,0.2,0.3,0.4,0.5 and y=0.05) were prepared by conventional standard ceramic technique. The single-phase cubic spinel structures of the samples were confirmed by x-ray diffraction patterns. It seems that substituted Sm^{3+} decreases the lattice constant by small extent and increases x-ray density. Lattice constant is found to decrease first upto x=0.1,beyond which it increases with Zn concentration x. The x-ray density is found to increase first upto x=0.1 and then after it decreases slowly. The hoping lengths L_A, L_B and bond lengths d_{Ax}, d_{Bx} are found varying as per changes in lattice constant. The cation distribution shows that non-magnetic Zn^{2+} occupies A-site. Ni^{2+} and Sm^{3+} are found to be diverting towards B-site. Lattice constant calculated theoretically from cation distribution is found higher than experimentally observed lattice constant. The substitution of Sm^{3+} increases the electrical resistivity of ferrites. The resistivity decreases with increasing temperature. The graphs between (logρ) and (1000/T) show two regions corresponding to paramagnetic and ferrimagnetic behaviour through straight lines. Curie temperature obtained by d. c. resistivity are in good compromise with those obtained by a. c. susceptibility. Activation energies are found greater in paramagnetic region than those in ferrimagnetic region.

Keywords: Polycrystalline ferrites, structural and electrical properties.

Introduction

Cobalt spinel ferrite, ($CoFe_2O_4$) has attracted attention of scientists and researchers because of their possible use in magneto-optical recording materials. According to literature survey cobalt ferrite is an inverse spinel ferrite whose degree of inversion depends upon the heat treatment. The conductivity in $CoFe_2O_4$ which has the cation distribution $(Fe^{3+})^A[Co^{3+}Fe^{3+}]^B$ O_4 can be attributed to high activation energy of the hopping mechanism because the hopping between ions of different metals is likely to be more highly activated than that of ions of same metal. Thus hole hopping between Co^{3+} and $Co^{2}+$ is predominant conduction mechanism in $CoFe_2O_4$. The hole hopping mechanism was also reported for other ferrites containing cobalt [1]. The control of resistivity in ferrites is a serious problem. There are two general approaches to this (1) controlling firing temperature and (2) addition of minor constituents to increase or decrease the conductivity. The physical properties of ferrites depend on the method of preparation and amount and type of dopant. The electron exchange interaction ($Fe^{2+}\leftrightarrow Fe^{3+}$) results in a local displacement of electrons during the sintering process of ferrites [2-5]. The electrical properties of La doped Co-Zn ferrites was also studied to see the effect of Zn dilution in the presence of rare earth ion(La^{3+}) on the electrical properties [6].

As $ZnFe_2O_4$ is a normal spinal ferrite [7-9] while $CoFe_2O_4$ is an inverse spinel ferrite [10-11], it is interesting to study the structural and electrical properties of Co-Zn ferrite doped with Sm^{3+}. The variation of ionic radii of the metal ions forming the spinel system will not vary the unit cell dimensions over a wide range because the stability of the spinel structure takes place only if cations (divalent and trivalent) are of

medium size [12]. The aim of the present investigation is to study the structural and electrical properties of samarium doped Co-Zn ferrite.

Experimental

All the samples of the system $Co_{1-x}Zn_xFe_{2-y}Sm_yO_4$ were prepared by standard double sintering ceramic method. The starting material oxides in A.R. grade used for the preparation of samples in this system were CoO, ZnO, Fe_2O_3, Sm_2O_3. These oxides were thoroughly mixed in one another and then ground for two hours till the fine powder is obtained. Then these powders were presintered at 900^0 C for 16 hours in a furnace and allowed to cool to room temperature. These samples were then pressed into pellets and pellets were finally sintered at 1100^0 C for 24 hours in the same furnace and cooled up to room temperature at the rate of 2^0C/min. These pellets were then the final products of the system. The phase purity of the samples was analysed by using X-ray diffraction method with Cu-Kα radiation. The d. c. electrical resistivity of all the samples was measured with the help of two probe method in the temperature range 300 K to 900 K.

Results and discussion

XRD Analysis

X-ray diffractograms of the ferrite series show the completion of the solid state reaction and the formation of cubic spinel compounds. The typical x-ray diffraction patterns of the samples x = 0, 0.2, 0.4 are shown in Fig 1. It is observed from this figure that there exists one small extra unidentified peak on the lower angle side of (311) plane. The appearance of such peak may be due to high reactivity at high temperature between Sm and Fe which results into the formation of perovskite phase. The similar phase was reported by J. L. Bhosale et. al. [13] in Mg-Cd ferrite substituted with Gd^{3+} ion. and by C. B. Kolekar et al. [14] in Gd^{3+} substituted Cu-Cd mixed ferrite. In all samples, the widths of half of maximum intensity peak of (311) planes are almost the same in magnitude, indicating that the substituents have occupied the corresponding lattice sites [15]. The observed peaks in all the samples are sharp and intense which confirms the formation of cubic spinel structure.

The interplaner spacing 'd' was calculated from Bragg's law $n\lambda = 2d \sin\theta$ and lattice constant 'a' was determined by using the relation $a = d\sqrt{N}$ where $N = h^2 + k^2 + l^2$ and — h, k, l are miller indices. The determined values of lattice constant 'a' are listed in Table 1 and variation of 'a' with Zn concentration 'x' in shown in Fig 2. The lattice constant of pure Co-ferrite is 8.380 Å [16]. In the present work for sample x=0 (i.e. for $CoFe_{1.95}Sm_{0.05}O_4$) it is found that lattice constant is 8.376 Å indicating that 'a' is decreased by 0.004 Å due to Sm^{3+} substitution in Co-Zn ferrite. From Table 1 it is seen that the lattice constant decreases initially up to x = 0.1 and then increases with Zn concentration 'x'. Due to introduction of Zn^{2+} ion lattice constant initially decreases up to x = 0.1. Then after lattice constant increases with increasing Zn concentration x. This is due to replacement of Co^{2+} ion of smaller ionic radia (0.78 Å) by Zn^{2+} ions of larger ionic radia (0.83 Å). X-ray density of each sample was calculated and the values are presented in Table 1. X-ray density of pure cobalt ferrite is 5.290 Å [16]. In our system for sample x = 0 (i.e. for $CoFe_{1.95}Sm_{0.05}O_4$) it is found that X-ray density is 5.410 Å. This means X-ray density is increased due to Sm^{3+} substitution in Co-Zn ferrite. X-ray density changes as per the variation of lattice constant with Zn concentration x. It is found that dx is decreased above the sample for which x = 0.1. The variation of x-ray density with Zn concentration 'x' is shown in Fig 2. The hopping lengths L_A and L_B on

both the sites are shown in Table 1 indicating that these values change as per the changes in lattice constant. The variation of L_A and L_B with Zn concentration x is shown in Fig 3. The relation between the ionic radia and lattice constant is given by [17]

$$a_{th} = \frac{8}{3\sqrt{3}}\left[(r_A + r_O) + \sqrt{3}(r_B + r_O)\right]$$ where r_A is ionic radius on tetrahedral (A) – site, r_B is ionic radius on Octahedral [B] – site and r_0 is ionic radius of oxygen (1.32 Å)

It is essential to know the cation distribution to calculate r_A and r_B. Depending upon the ionic radia and site preference of constituent ions cation distribution is confirmed. Among the few combinations made to study the cation distribution, one such combination is choosed which shows the nearest difference between observed and calculated x-ray intensity ratios for the planes (220), (400) and (422), (440) as these planes are structure sensitive [18]. The assumed cation distribution is shown in Table 2 which shows that Zn^{2+} resides at tetrahedral (A) site and Sm^{3+}, Co^{2+} at octahedral [B] site whereas Fe^{3+} occupies both sites. Ionic radia r_A, r_B were calculated from cation distribution and the values are listed in Table 3. The variation of r_A and r_B with Zn concentration x is depicted in Fig 4. It is noticed from this figure that r_A increases and r_B decreases with x.

The introduction of Zn^{2+} ions of larger ionic radia (0.83Å) instead of Fe^{3+} ions of smaller ionic radia (0.67 Å) increases r_A. On the other hand because of migration of Fe^{3+} ions to B site r_B decreases due to increasing concentration of Fe^{3+} ions of smaller ionic radia. Decrease in r_B can also be attributed to decreasing concentration of Co ions of larger ionic radia (0.78 Å). The lattice constant was calculated theoretically and the values are shown in Table 3. It is observed that a_{th} is higher than a_{exp} for all the concentration. The variation of a_{th} with Zn concentration x is shown in Fig 5. Bond lengths on both tetrahedral (A) and octahedral [B] sites are determined by using u parameter as given in the following relation (for Ni, u = 0.381 Å)

$$d_{AX} = \left(u - \frac{1}{4}\right) a\sqrt{3}$$

$$d_{BX} = a \times \sqrt{\left(3u^2 - \frac{11}{4}u + \frac{43}{64}\right)}$$

The determined values of bond lengths on A site (tetrahedral bond) and B site (octahedral bond) are shown in Table 4. It is seen from table that bond lengths of both the sites are decreased up to x = 0.1 and then increased for higher concentration of Zn. This increase is due to increase in lattice constant. The lattice edges on both the sites are also computed with the help of following formulae,

$$d_{AE} = \left(2u - \frac{1}{2}\right) a\sqrt{2}$$

$$(d_{BE})_{shared} = (1 - 2u)\, a\sqrt{2}$$

$$(d_{BE})_{unshared} = a \times \sqrt{\left(4u^2 - 3u + \frac{11}{16}\right)}$$

The computed values of tetrahedral edge, octahedral edge (shared) and octahedral edge (unshared) are given in the Table 4. By observation of the table we see that the values of tetrahedral and octahedral edges are decreased up to x = 0.1 and then after they go on increasing because of increasing lattice constant.

DC resistivity

The resistivity □ was calculated using the relation.

□ = □$_0$ exp (-□E / kT) where, □$_0$ is temperature independent constant,

□E is activation energy,

k is Boltzman constant. The variation of resistivity with temperature for all the samples is shown in Fig. 6(a) and 6 (b). It is clear from these figures that as temperature increases, resistivity decreases. The variation of resistivity with Zn concentration x at fixed temperature

503 K, 603 K and 703 K is shown in Table 3. From this table is clear that for a fixed temperature, The resistivity is decreased initially up to the sample x = 0.1 and then it is found increasing with increasing Zn concentration x. The variation of resistivity at fixed temperature 703 K with Zn concentration x is shown in Fig 7. The typical graphs of logarithm of resistivity (log □ and reciprocal of temperature (1000/T) for the samples x = 0, 0.1, 0.2, 0.3 are plotted and shown in the Fig 8(a), 8(b). From these figures we observe that the nature of each graph is linear up to certain transition temperature known as curie temperature, beyond which graph changes its slope and becomes linear again. At the Curie temperature ferrimagnetic samples change over to a paramagnetic state due to influence of magnetic ordering upon conductivity process in ferrite. The plots are hence divided into two regions at T_c, into ferrimagnetic region and paramagnetic region. The region of plot below T_C is called ferrimagnetic region while above T_C it is called paramagnetic region. T_C of all samples are shown in Table 5. From this table it is found that T_C goes on decreasing with increase in Zn concentration x. The variation of Tc with x is shown in Fig 9. Activation energies of all samples for both the regions of plots are determined and presented in Table 5, which shows that activation energy for paramagnetic region is greater than that of ferrimagnetic region. The similar behavior of log □ verses (1000/T) plots is observed for other spinels. The difference between activation energies of paramagnetic region and ferrimagnetic region gives the resultant activation energies of samples, which are given in the same Table 5. The conduction in paramagnetic region is explained as an impurity conduction, while that in ferrimagnetic region is due to polaron hoping from Fe^{3+} to Fe^{2+} on the B-site [19]. Already it is reported that if substituted ion occupies B-site then the effect on activation energy is greater [20] whereas if it occupies A-site without disturbing B-site, then activation energy almost remains unaltered [21]. Also it is reported that hoping between ions of different metals on B site requires higher value of activation energy than for ions of same metal [22]. In the present work Zn^{2+} ions have a preference to A-site so that they cannot take part in affecting activation energy (A. E.) therefore change in A. E. can be attributed to Sm^{3+} occupying octahedral [B] site.

Conclusion

The investigations of the system $Co_{1-x} Zn_x Fe_{2-y} Sm_y O_4$ leads to the following conclusions.

1. Lattice Constant is found to decrease slightly and X-ray density is found to increase due to substitution of Sm^{3+}. Also it is found that lattice constant increases from x = 0.1 and x-ray density decreases with increase in Zn concentration x.
2. As per cation distribution it is noticed that Zn diverts to A site and Co, Sm resides on B-site. Fe occupies both A & B sites.
3. Ionic radii r_A goes on increasing while r_B goes an decreasing with increase in Zn concentration x.
4. Theoretically calculated lattice constant is found greater than experimentally observed lattice constant.
5. The resistivity decreases with increasing temperature. The graphs between (log) and (1000/T) show two regions corresponding to paramagnetic and ferrimagnetic behaviour through straight lines. Curie temperatures obtained by d. c. resistivity are in good compromise with those obtained by a. c. susceptibility. Activation

energies are found greater in paramagnetic region than those in ferrimagnetic region.

REFERENCES

[1] R. M. Gillot, G. Benloucif, A. Rousset Phys. Stat. Sol. A 65 (1981) 205.

[2] O. S. Josyulu, J. Sobhanadri Phys. Stat. Sol. (a) 59 (1980) 323.

[3] S. A. Mazen, A. E. Abd El-Rahim J. Matt. Sci. 23 (1988) 2917.

[4] M. S. Ramana J. Matt. Sci. Lett. 3 (1984) 1049.

[5] S. Phanjoubam, D. Kothari, J. S. Baijal Phys. Sol (a) 111 (1989) 131

[6] Abedellatif Indian J. phys. 77 A (4) (2003) 359.

[7] H. N. Ok and B. J. Evens Phys. Rev. B. 14 (1976) 2956.

[8] D. C. Dobson, J. W. Linnet and M. M. Rehman J. Phys Chem Soli. 31 (1970) 2727.

[9] H. Tang, Y. W. Du, Z. Q. Qiu and J. C. Walker J. Appl. Phys. 63 (1988) 4105.

[10] H. M. Vanoort, J. W. D Marteens and W. L. Peeters Matt. Res. Bull 20 (1985) 41.

[11] V. R. Murthy and J. Sobhanadri Phys. Status sol. (a) 36 (1976) k 133

[12] M. A. Ahmed and M. H. Wasfy Ind. J. of Pure and App. Phys. Vol 41 (2003) 731 J. M. M. M. 219 (2000)9.

[13] J.L. Bhosale, S.N. Kulkarni, R.B. sasmile and B. K. Chougule Bull Matt. Sci 19 No 5 (1996) 767.

[14] C. B. Kolekar, P. N. Kamble and A. S. Vaingankar J.M.M.M.138 (1994) 211.

[15] K. Suzuki, T. Namikawa, Y. Yamazak Jpn. J. Appl. Phys 27 (1988) 361.

[16] R. S. Tibble, D. J. Craik “Magnetic Materials”

[17] S. A. Mazen, M. H. Abdellah, B. A. Sabrah, H. A.M. Hashem, Phys stat. Sol. A 134 (1992) 263.

[18] H. Ohnishi and T. Teranishi J. Phy. Soc. Japan 16 (1961) 36.

[19] E. L. J. verwey and E. W. Hayman J. chem. Phys 15(1947) 1218.

[20] M. A. Ahmed, A. Tawfik, M. K. El-Nimr and A. A. El-Hasab J. Matt. Sci. 10 (1991) 549

[21] A. B. Dewale, Ph. D. Thesis, Institute of Science, Nagpur University, India (1980).

[22] C. C. Wu, S. Kumarkrishna and T. O. Mason J. Solid state Chem. 37 (1981) 144.

Table 1-

Compo.	dAX	dBX	Edges		
'x'			Tetra edge	Octa edge dBXE	
			dAXE	Shared	unshared
0	1.901	2.044	3.103	2.819	2.963
0.1	1.894	2.037	3.093	2.809	2.952
0.2	1.898	2.042	3.1	2.815	2.959
0.3	1.899	2.043	3.101	2.817	2.961
0.4	1.901	2.045	3.105	2.82	2.964
0.5	1.902	2.045	3.106	2.821	2.965

Table 2-

Comp.	'a'	'dx'	LA	LB
'x'	(Å)	(gm/cm3)	(Å)	(Å)
0	8.376	5.41	3.627	2.961
0.1	8.347	5.481	3.614	2.951
0.2	8.367	5.457	3.623	2.958
0.3	8.371	5.463	3.625	2.959
0.4	8.38	5.46	3.629	2.962
0.5	8.383	5.47	3.63	2.963

Table 3-

	'rA'	'rB'	'ath'	d.c. resistivity in W m		
'x'	(Å)	(Å)	(Å)	503K	603K	703K
0	0.692	0.721	8.541	373	215	134
0.1	0.714	0.713	8.552	156	62	28
0.2	0.735	0.705	8.563	662	258	104
0.3	0.757	0.697	8.574	3310	1130	409
0.4	0.778	0.688	8.585	4069	1383	550
0.5	0.8	0.68	8.596	15617	6594	2135

Table 4-

Comp.	'Tc'	Activation energy in (eV)		
'x'	(K)	Ep	Ef	$-\pi E = E\Delta\ \phi E$
0	690	0.198	0.132	0.066
0.1	667	0.273	0.199	0.074
0.2	588	0.325	0.176	0.149
0.3	526	0.331	0.258	0.073
0.4	513	0.317	0.176	0.141
0.5	455	0.238	0.17	0.068

Table 5-

x	A – site		B - site		
	Zn	Fe	Co	Fe	Sm
0	0	1	1	0.95	0.05
0.1	0.1	0.9	0.9	1.05	0.05
0.2	0.2	0.8	0.8	1.15	0.05
0.3	0.3	0.7	0.7	1.25	0.05
0.4	0.4	0.6	0.6	1.35	0.05
0.5	0.5	0.5	0.5	1.45	0.05

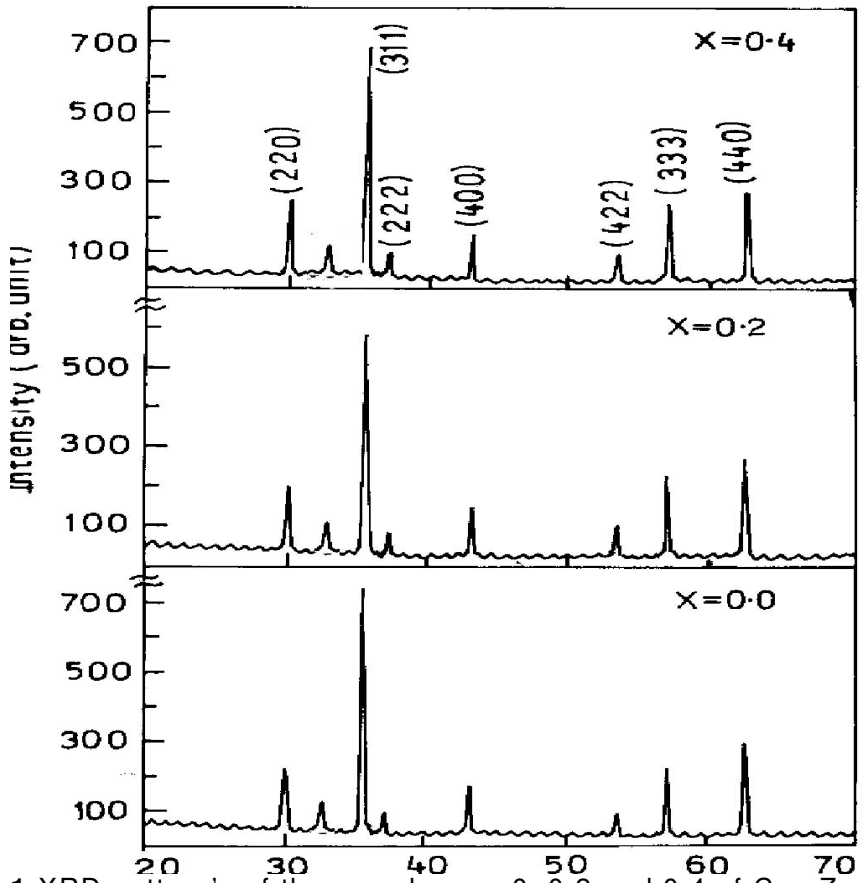

Fig. 1-XRD pattern's of the samples x = 0, 0.2 and 0.4 of $Co_{1-x}Zn_xFe_{2-y}Sm_yO_4$

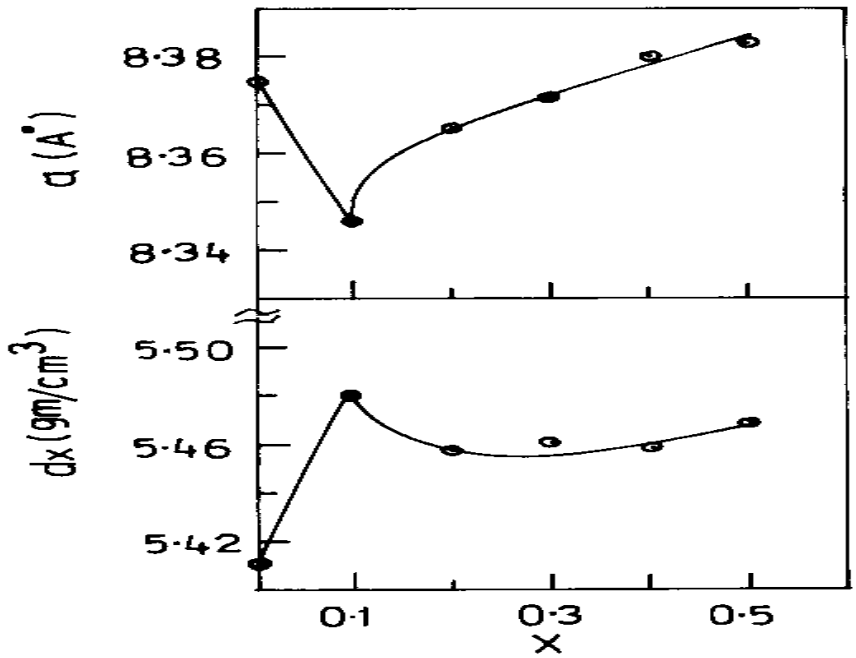

Fig. 2- Variation of lattice constant and X-ray density with concentration 'x' of the system $Co_{1-x}Zn_xFe_{2-y}Sm_yO_4$

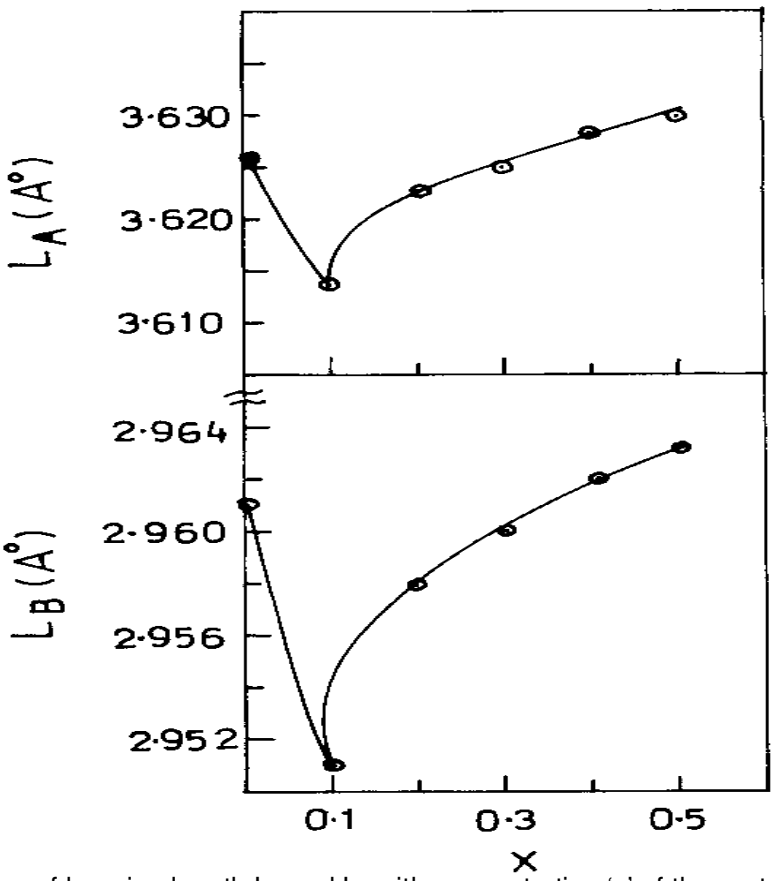

Fig. 3-Variation of hopping length L_A and L_B with concentration 'x' of the system $Co_{1-x}Zn_xFe_{2-y}Sm_yO_4$

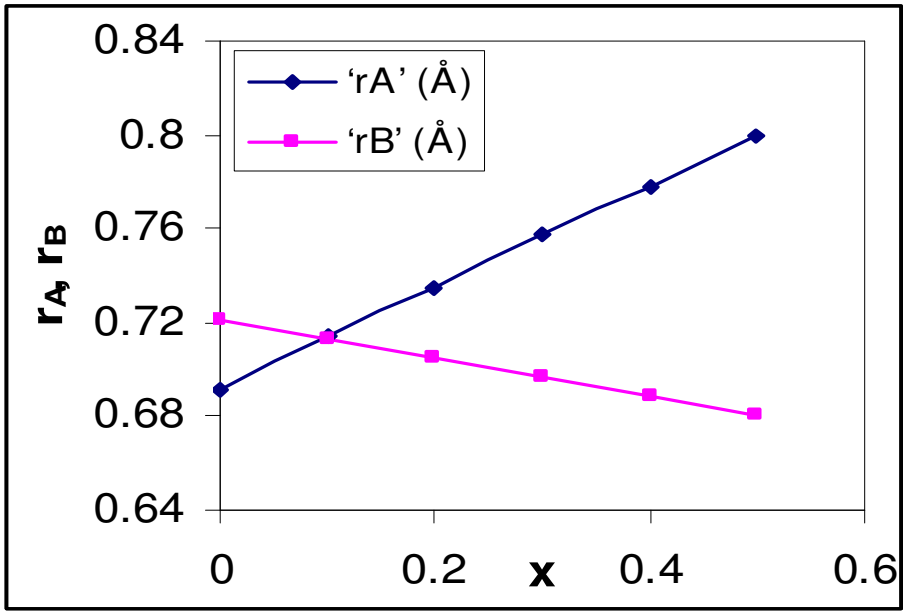

Fig. 4-Variation of ionic radii r_A, r_B with concentration 'x'

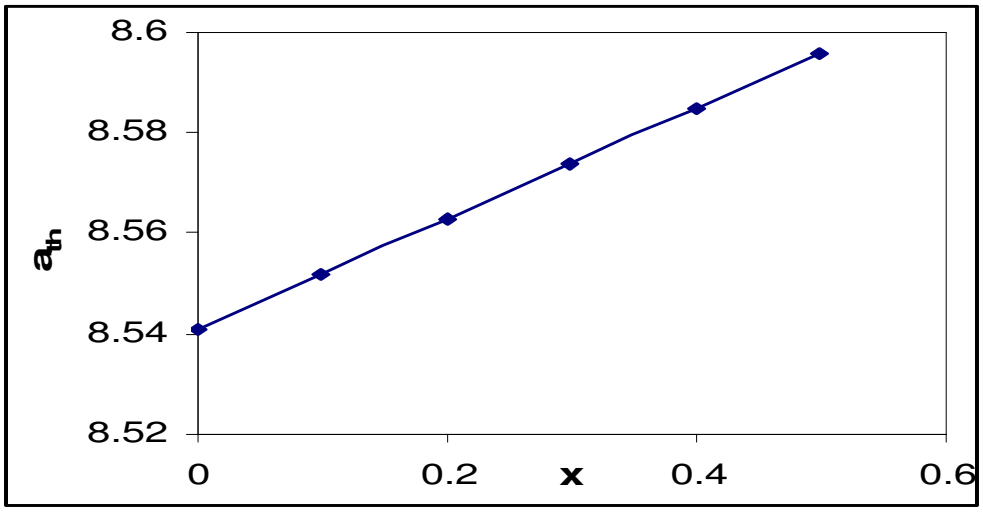

Fig. 5-Variation of theoretical lattice constant calculated from cation distribution with Zn concentration 'x'

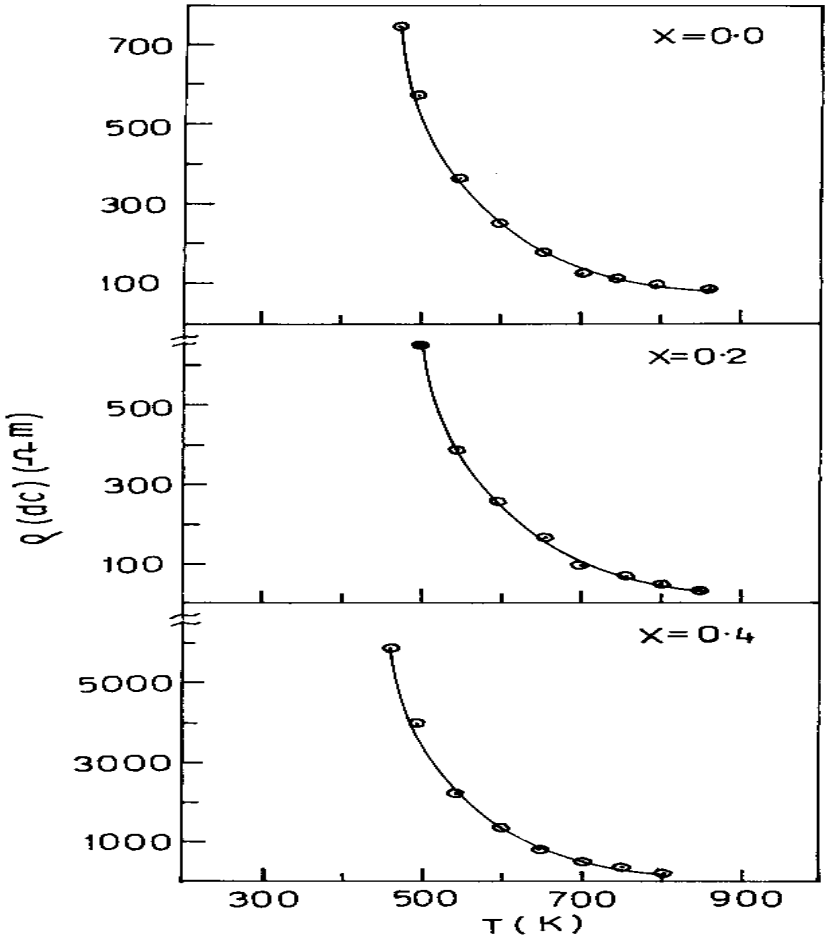

Fig. 6a-Variation of d.c. resistivity (ρ) with temperature (T) for x = 0.0, 0.2 and 0.4 of the system $Co_{1-x}Zn_xFe_{2-y}Sm_yO_4$

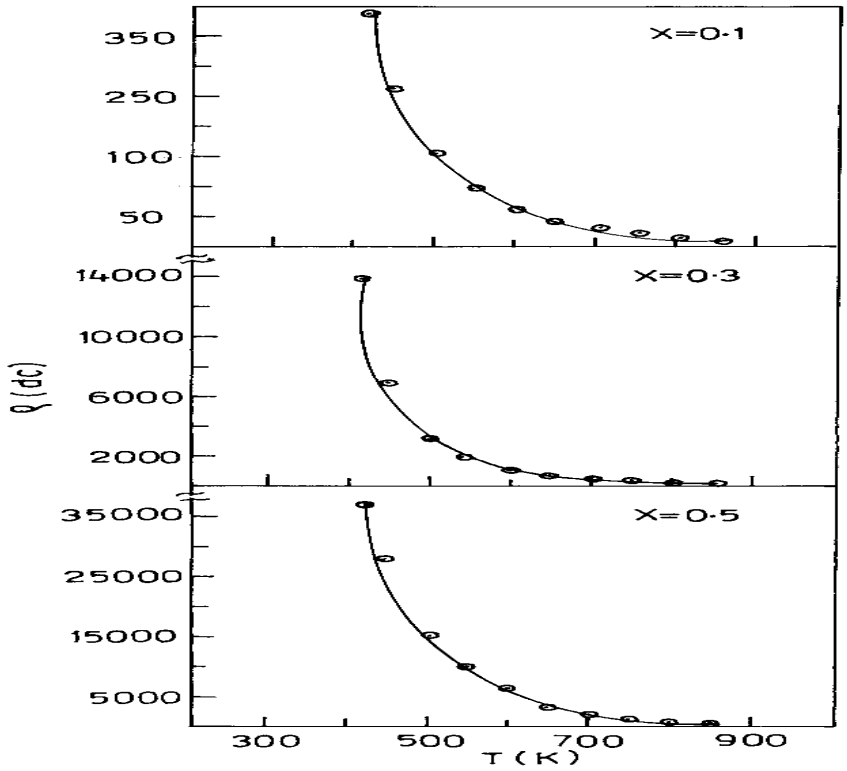

Fig. 6b- Variation of d.c. resistivity (ρ) with temperature (T) for x = 0.1, 0.3 and 0.5 of the system $Co_{1-x}Zn_xFe_{2-y}Sm_yO_4$

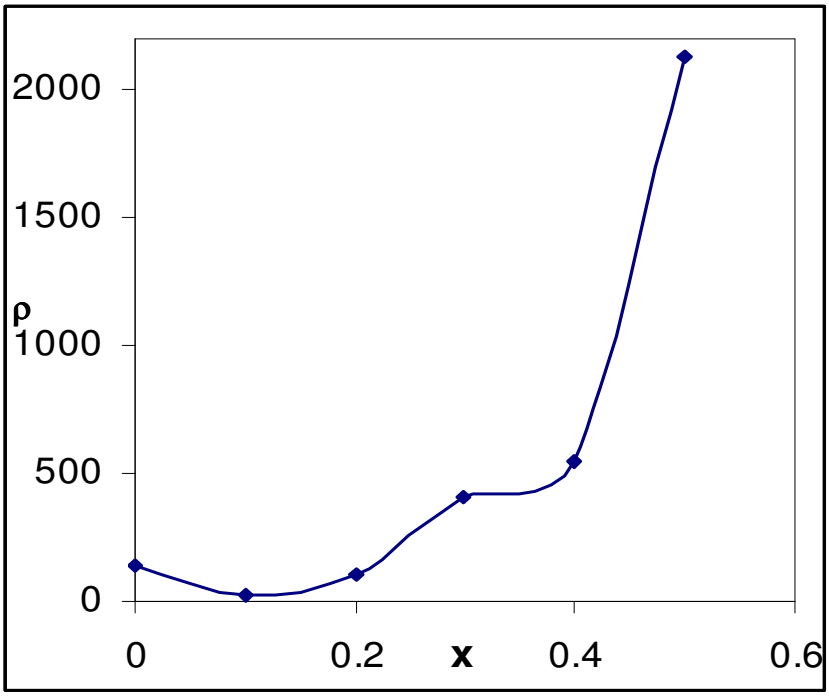

Fig. 7-Variation of resistivity at fixed temperature 703 K with concentration 'x'

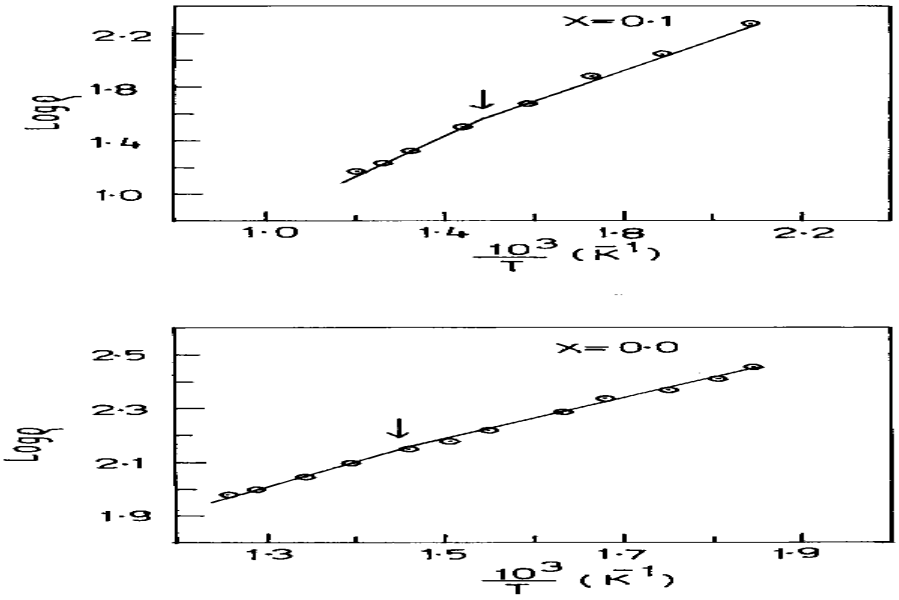

Fig. 8a-Variation of (log ρ) with (1000/T) for x = 0.0 and 0.1 of the system $Co_{1-x}Zn_xFe_{2-y}Sm_yO_4$

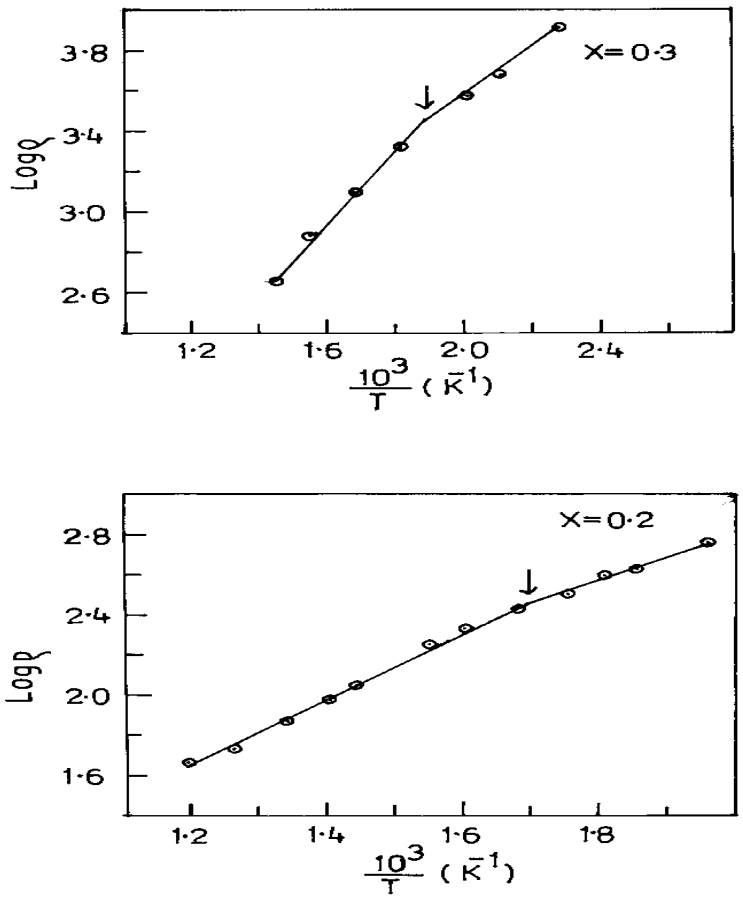

Fig. 8b-Variation of (log ρ) with (1000/T) for x = 0.2 and 0.3 of the system $Co_{1-x}Zn_xFe_{2-y}Sm_yO_4$

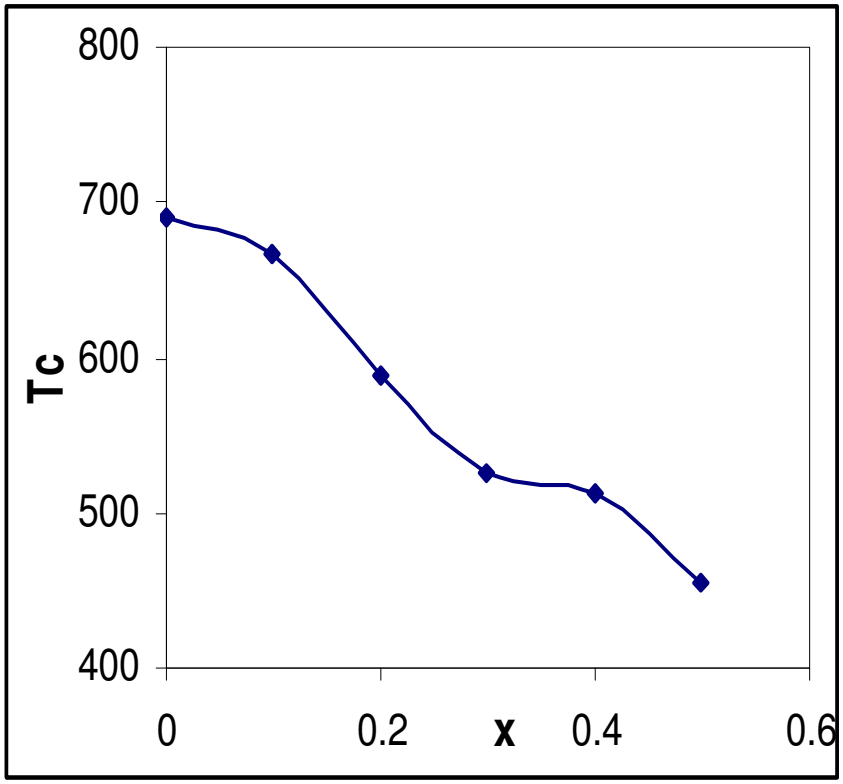

Fig. 9-Variation of Curie temperature Tc with 'x' of the system $Co_{1-x}Zn_xFe_{2-y}Sm_yO_4$